Steel and Composite Structures, *Vol. 24, No. 5 (2017) 537-548*
DOI: https://doi.org/10.12989/scs.2017.24.5.537

Bending behavior of SWCNT reinforced composite plates

Shivaji G. Chavan [a] and Achchhe Lal [*]

Department of Mechanical Engineering, S.V. National Institute of Technology, Surat - 395007, India

(*Received July 02, 2016, Revised March 31, 2017, Accepted May 08, 2017*)

Abstract. In this paper presents bending characteristic of single wall carbon nanotube reinforced functionally graded composite (SWCNTRC-FG) plates. The finite element implementation of bending analysis of laminated composite plate via well-established higher order shear deformation theory (HSDT). A seven degree of freedom and C^0 continuity finite element model using eight noded isoperimetric elements is developed for precise computation of deflection and stresses of SWCNTRC plate subjected to sinusoidal transverse load. The finite element implementation is carried out through a finite element code developed in MATLAB. The results obtained by present approach are compared with the results available in the literatures. The effective material properties of the laminated SWCNTRC plate are used by Mori-Tanaka method. Numerical results have been obtained with different parameters, width-to-thickness ratio (a/h), stress distribution profile along thickness direction, different SWCNTRC-FG plate, boundary condition, through the thickness (z/h) ratio, volume fraction of SWCNT.

Keywords: SWCNTRC plate; micromechanics model; HSDT; FEM formulation

1. Introduction

The single walled carbon nanotube (SWCNT) composite reinforced broadly applied in the field of mechanical, civil, aerospace industries, missile, automobile and many other industries. The SWCNT composite falls in the category of advanced material. Higher strength at lower weights, close control over mechanical properties and simultaneous advancement of manufacturing technology have given an edge to composite materials over their metallic counterparts in bright applications. To reduce the time span for design of light and safe systems which meet rigorous functional requirements, there is a need for accurate and realistic failure analysis tools. Finite element implementation for bending analysis of composites has been a strong alternative to experimental testing during recent years because of cost and time factor.

The molecular dynamic model and Finite Element Method (FEM) nanotube composite plate was studied by Wattanasakulpong and Chaikittiratana 2015) lead simulate for static and dynamic analysis. Third order shear deformation theory (TSDT) plate, classical laminated plate theory (CLPT) disreputable on the assumption of and first order shear deformation plate theory (FSDT) were presented by Rastgaar Aagaah *et al*. (2014). Bhashyam and Gallagher (1983) presented Multi-scale analysis nominated as origin to evaluated deflection and stresses of SWCNTRC plate by effect of volume fraction, aspect ratio (a/h), thickness ratio (z/h). Wuite (Wuite and Adali 2005) and Zhu *et al*. (2012) studied static and dynamic analyses of carbon nanotube-reinforced composite plates using finite element method with first order shear deformation plate theory. Bending responses of laminated SWCNT reinforced composite plate anticipate as perfect bonded was explained by Reddy *et al*. (2012). The governing differential equation of bending behavior of laminated CNTRC plate using element free Ritz method was presented by Lei (Lei *et al*. 2013). They also studied effect of the volume fraction of SWCNT, aspect ratio (a/h) and thickness ratio (z/h) on laminated functional distributed of SWCNTRC Plate. Lei *et al*. (2013) presented load transfer and deformation mechanism in SWCNT- polyester composite and originated that additions of only 1wt.% SWCNT results in 36.42%-42% of 25% increase in elastic modulus as well as break stress. Kreculj (2008) estimated the electrical resistivity and complex viscosity properties improved by added SWCNT.

Hu *et al*. (2010) evaluated the elastic properties by using micromechanics models and Molecular dynamics simulation of SWCNTRC plate. Mohammadpour *et al*. (2014) presented finite element modeling for stress-strain response of carbon nanotube Nano composites using nonlinear representative volume element. Han (Han and Elliott 2007) studied micro-mechanics model such as helpin-Tesai and Mori-Tanka for evaluation of mechanical property of carbon nanotube composite plate. Concept of bending and free vibration analysis of using finite element method scrutinizes by the SWCNTR functional graded composite plates was presented by Zhang *et al*. (2014). Salami (2016) studied bending analysis of sandwich beam with soft and carbon nano tube reinforced composite face sheets based on Extended Higher order Sandwich Panel Theory (EHSAPT). Herasati *et al*. (2014) presented bending response the functional graded SWCNT reinforced composite plate. Reddy (1984) developed a simple higher order theory for laminated composite plates.

*Corresponding author, Assistant Professor,
E-mail: shivajigchavan@gmail.com
[a] Ph.D., Research Scholar

ISSN: 1229-9367 (Print), 1598-6233 (Online)

The nonlinear cylindrical bending behavior of functionally graded nano-composite plates reinforced by single-walled carbon nanotubes (SWCNTs) was studied by Bakhti *et al*. (2013). Rupp *et al*. (2014) developed a new concrete confinement model to predict the axial load versus displacement behavior of circular columns under concentric axial load. Mehditabar *et al*. (2014) investigated magneto-thermo-elastic thick truncated conical shell immersed in a uniform magnetic field and subjected to internal pressure. Prokic *et al*. (2014) developed for the determination of geometrical and material properties of composite thin-walled beams with arbitrary open cross-section and any arbitrary laminate stacking sequence. Bending analysis of sandwich structures with flexible cores subjected to concentrated load, uniform distributed load on a patch, harmonic and uniform distributed loads on the top and/or bottom face sheet of the sandwich structure was investigated by Fard (2015). Thirumalaiselvi *et al*. (2016) presented the numerical evaluation of deformation capacity of laced steel-concrete composite beams under monotonic loading. Bounouara *et al*. (2016) studied a nonlocal zero-order shear deformation theory for free vibration of functionally graded Nano scale plates resting on elastic foundation.

A New high-order simple-input analytical method used to study thick laminated composite straight tubes subjected to combined axial force, torque and bending moment were investigated by Sarvestani and Hojjati (2016). Kara *et al*. (2016) an investigated of anchorage to the edge of steel plates bonded to RC structures. They also studied the results of an experimental study the effects of anchorage systems used in externally bonded steel plates on the strength and ductility of reinforced concrete structures. Houari *et al*. (2016) developed a new simple higher-order shear deformation theory for bending and free vibration analysis of functionally graded (FG) plates.

Free vibration, forced vibration, resonance and stress wave propagation behaviour in Nano-composite plates reinforced by wavy carbon nanotube (CNT) by using a mesh-free method based on first order shear deformation theory (FSDT) were studied by Moradi-Dastjerdi and Momeni-Khabisi (2016). Hadianfard and Khakzad (2016) investigated the buckling and post-buckling behavior of bracing gusset plates by using finite element non-linear static analysis and comparing it with experimental models. Wu *et al*. (2016) studies the seismic behavior of reinforced concrete (RC) walls with encased cold-formed and thin-walled (CFTW) steel truss. Hebali *et al*. (2016) presented bending, buckling, and vibration analysis of functionally graded plates by employing a novel higher-order shear deformation theory (HSDT).

However most of the researchers have attempted these types of problem by using FSDT and classic laminated plate theory and ANSYS software. It is accomplished from the above mentioned literatures that the finite element formulation of bending analysis in conjunction with HSDT. The different configuration of SWCNT has not reported in above literatures. The main objective of the present research is aimed to evaluate bending behaviour of SWCNTRC plate. In the present study, the higher order shear deformation theory is used to bending behaviour of SWCNTRC plate. For SWCNTRC plate both cases of uniform (UD) and functional graded (FG) distribution pattern of SWCNT reinforcement are considered. Micromechanics approach is used in order to obtain the effective material properties of SWCNTR-FG plate. The details parametric studies are carried out to investigate the effect of SWCNT volume fraction, plate width-to-thickness ratio, plate thickness ratio (z/h), chirality index and boundary condition on bending response of SWCNTRC-FG plates.

2. Micromechanics analysis

The effective material properties of SWCNTRC plate are obtained by using Mori-Tanaka model (Huang *et al*. 2004). The carbon nanotube composite plate is made up of matrix Epon 862 and SWCNT. The bonding of SWCNT and matrix is taken to be perfect. The stress and strain constitute equation is expressed as

$$\begin{bmatrix}\sigma_{11}\\ \sigma_{22}\\ \sigma_{33}\\ \sigma_{23}\\ \sigma_{13}\\ \sigma_{12}\end{bmatrix}=\begin{bmatrix}n & l & l & 0 & 0 & 0\\ l & k+m & k-m & 0 & 0 & 0\\ l & k-m & k+m & 0 & 0 & 0\\ 0 & 0 & 0 & 2m & 0 & 0\\ 0 & 0 & 0 & 0 & 2p & 0\\ 0 & 0 & 0 & 0 & 0 & 2p\end{bmatrix}\begin{bmatrix}\varepsilon_{11}\\ \varepsilon_{22}\\ \varepsilon_{33}\\ \varepsilon_{23}\\ \varepsilon_{13}\\ \varepsilon_{12}\end{bmatrix} \tag{1a}$$

Where, k, l, m, n and m are hill elastic constant's is uni-axial tension modulus in the fiber direction, k is plane-strain bulk modulus normal to fiber direction. l, is associated cross modulus, m and p is shear modulus in planes normal and parallel to fiber direction respectively. The Mori-Tanaka Method is used in the present study because of its simplicity and accuracy at a high volume fraction of carbon nanotube as inclusion. Assumed that each inclusion is surrounded in an infinite matrix subjected to effective stress (σ_{avg}) or strain (ε_{avg}). Where σ_{avg} and ε_{avg} is average stress and strain of matrix respectively. The tensor of effective elastic modulus of SWCNTRC can be defined as

$$C=\left(V_m H_m+V_{CNT}H_{CNT}:A\right):\left(V_m I+V_{CNT}A\right)^{-1} \tag{1b}$$

H_m and H_{CNT} is tensor of elastic modulus of the corresponding phases. V_m and V_{CNT} is volume fraction of matrix and SWCNT respectively. I is forth order identity tensor, A is fourth order average stress or strain expressed as

$$A=[\mathrm{I}+\mathrm{S}:{H_m}^{-1}:(H_{CNT}-H_m)]^{-1} \tag{2}$$

Where, S is Eshelby tensor for straight long SWCNT

$$S_{1111}=S_{3333}=\frac{5-4v_m}{8(1-v_m)},$$
$$S_{1122}=S_{3322}=\frac{v_m}{2(1-v_m)}, \tag{3}$$

$$S_{1133} = S_{3311} = \frac{4v_m - 1}{8(1-v_m)};$$

$$S_{2323} = S_{1212} = \frac{1}{4}; \quad S_{1313} = \frac{3-4v_m}{8(1-v_m)}$$

A-Tensor as

$$A_{1111} = A_{3333} = -\frac{C_3}{C_1C_2}, \quad A_{1133} = A_{3311} = \frac{C_4}{C_1C_2};$$

$$A_{1122} = A_{3322} = \frac{l_{CNT}(1-v_m-2v_m^{\,2}) - \mathrm{E}_m v_m}{C_1} \quad A_{2222} = 1; \quad (4)$$

$$A_{2323} = A_{1212} = \frac{\mathrm{E}_m}{\mathrm{E}_m + 2p_{CNT}(1+v_m)}; A_{1313} = \frac{2\,\mathrm{E}_m(1+v_m)}{C_2}$$

Here

$$C_1 = (-1+2v_m)[\mathrm{E}_m + 2k_{CNT}(1+v_m)];$$

$$C_2 = \mathrm{E}_m + 2m_{CNT}(3-v_m-4v_m^{\,2})$$

$$C_3 = \mathrm{E}_m(1-v_m)\{\mathrm{E}_m(3-4v_m)+2(1+v_m) \\ [m_{CNT}(3-4v_m)+k_{CNT}(2-4v_m)]\} \quad (5)$$

$$C_4 = \mathrm{E}_m(1-v_m)\{\mathrm{E}_m(1-4v_m)+2(1+v_m) \\ [m_{CNT}(3-4v_m)+k_{CNT}(2-4v_m)]\}$$

k_{CNT}, l_{CNT}, n_{CNT}, m_{CNT} and p_{CNT} are the hills elastic constant, the hills elastic can be defined as

$$k_{CNT} = \frac{E_{22}^{CNT}}{2(1-v_{23}^{CNT}-2v_{12}^{CNT}v_{21}^{CNT})};$$

$$l_{CNT} = \frac{v_{21}^{CNT}E_{11}^{CNT}}{(1-v_{23}^{CNT}-2v_{12}^{CNT}v_{21}^{CNT})} = \frac{v_{12}^{CNT}E_{22}^{CNT}}{(1-v_{23}^{CNT}-2v_{12}^{CNT}v_{21}^{CNT})} \quad (6a)$$

$$n_{CNT} = \frac{(1-v_{23}^{CNT})E_{11}^{CNT}}{(1-v_{23}^{CNT}-2v_{12}^{CNT}v_{21}^{CNT})}, \qquad p_{CNT} = G_{12}^{CNT}{}_{12} \\ m_{CNT} = G_{23}^{CNT}$$

The hill elastic constant is substitute Eq. (6a) into Eqs. (4)-(5) and calculate A-Tensor. Now Eq. (2), Eqs. (3) and (4) are substitute in Eq. (1b) for calculate C matrix. Compare Eqs. (1b) and (1a) will get exact values of Hills elastic moduli.

$$k = \frac{E_m\{E_mV_m + 2k_{CNT}(1+v_m)[1+V_{CNT}(1-2v_m)]\}}{2(1+v_m)[E_m(1+V_{CNT}-2v_m)+2V_mk_{CNT}(1-v_m-2v_m^2)]}$$

$$l = \frac{E_m\{V_mv_m[E_m+2k_{CNT}(1+v_m)]+2V_{CNT}l_{CNT}(1-v_m^2)\}}{(1+v_m)[E_m(1+V_{CNT}-2v_m)+2V_mk_{CNT}(1-v_m-2v_m^2)]}$$

$$n = \frac{E_m^2V_m(1+V_{CNT}-V_mv_m)+2V_mv_{CNT}(k_{CNT}n_{CNT}-l_{CNT}^2)(1-2v_m)}{(1+v_m)[E_m(1+V_{CNT}-2v_m)+2V_mk_{CNT}(1-v_m-2v_m^2)]} \\ + \frac{E_m[2V_m^2k_{CNT}(1-v_m)+V_{CNT}n_{CNT}(1-2v_m+V_{CNT})-42V_ml_{CNT}v_m]}{2V_mk_{CNT}(1-v_m+v_m^2)+E_m(1-V_{CNT}+2v_m)} \quad (6b)$$

$$p = \frac{E_m[E_mV_m+2(1+V_{CNT})p_{CNT}(1+v_m)]}{2(1+v_m)[E_m(1+V_{CNT})+2V_mp_{CNT}(1+v_m)]}$$

$$m = \frac{E_m[E_mV_m+2m_{CNT}(1+v_m)(3+V_{CNT}-4v_m)}{2(1+v_m)\{E_m[(V_m+4V_{CNT}(1-v_m)]+2V_mm_{CNT}(3-v_m-4v_m^2)]\}}$$

The elastic modulus of SWCNTRC plat is given by

$$E_{11} = n - \frac{l^2}{k}; \quad E_{22} = \frac{4m(kn-l^2)}{kn-l^2+mn}; \quad G_{12} = 2p; v_{12} = \frac{l}{2k} \quad (7)$$

In this study consider the SWCNTRC plate with five configurations of SWCNT RC plates as shown in Fig. 1. The mathematically model for functionally Graded SWCNTRC-FG plates, can be expressed as (Lei *et al*. 2013)

$$V_{CNT} = V^* \quad \text{----------} \quad \text{UD}$$

$$V_{CNT} = 2\left(1-\frac{2|z|}{h}\right)V^* \quad \text{----------} \quad \text{FG-O}$$

$$V_{CNT} = \left(\frac{2|z|+h}{h}+\right)V^* \quad \text{----------} \quad \text{FG-V} \quad (8)$$

$$V_{CNT} = 4\left(\frac{|z|}{h}+\right)V^* \quad \text{----------} \quad \text{FG-X}$$

$$V_{CNT} = 4\left(1-\frac{2|z|}{h}\right)V^* \quad \text{----------} \quad \text{FG-}\Delta$$

3. Seven degree of finite element formulation

In the present work, finite element formulation for SWCNTRC plate is based on HSDT because it represents

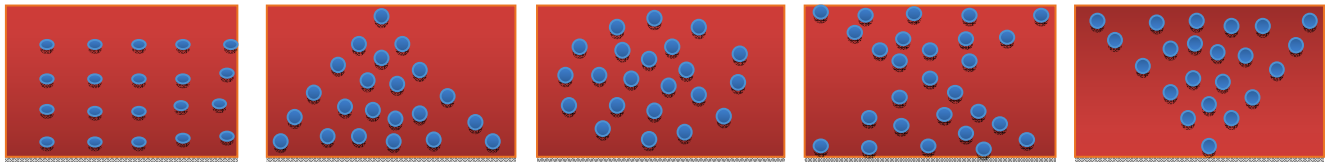

(a) UD plate (b) FG-A plate (c) FG-O plate (d) FG-X plate (e) FG-V plate

Fig. 1 Configurations of SWCNTRC-FG composite plates

the kinematics better, not require shear correction factors, and can yield more accurate stress distributions (Reddy 1984).

3.1 The displacement field

The origin of the material coordinates is in the middle of the SWCNTRC as shown in Fig. 2; the displacement field is given by

$$\begin{aligned}\bar{u}(x,y,z) &= u(x,y) + z\psi_x(x,y) + z^2\xi_x(x,y) + z^3\xi_x(x,y)\\ \bar{v}(x,y,z) &= v(x,y) + z\psi_y(x,y) + z^2\xi_y(x,y) + z^3\xi_y(x,y)\\ \bar{w}(x,y,z) &= w(x,y)\end{aligned} \quad (9)$$

u, v and w is displacement of point (x, y) on the mid plain Ψ_x and Ψ_y are the rotations of normal to mid plane about the y and x axes respectively. The functions ξ_x and ζ_y will be determined using the condition that the transverse shear stresses $\sigma_{xz} = \sigma_5$ and $\sigma_{yz} = \sigma_4$ vanish on the plate top and bottom surfaces.

$$\sigma_5 = (x,y,\pm h/2) = 0 \quad \text{and} \quad \sigma_4 = (x,y,\pm h/2) = 0 \quad (10)$$

For orthotropic plates, these conditions are equivalent to the requirement that the corresponding strains be zero on these surfaces.

Here

$$\begin{aligned}\varepsilon_5 &= \partial u/\partial z + \partial w/\partial x = \psi_x + 2z\xi_x + 3z^2\xi_x + \partial w/\partial x;\\ \varepsilon_4 &= \partial v/\partial z + \partial w/\partial y = \psi_y + 2z\xi_y + 3z^2\xi_y + \partial w/\partial y\end{aligned} \quad (11)$$

We obtained

$$\xi_x = -\frac{4}{3h^2}\left(\frac{\partial w}{\partial x} + \psi_x\right) \quad \text{and} \quad \xi_y = -\frac{4}{3h^2}\left(\frac{\partial w}{\partial y} + \psi_y\right) \quad (12)$$

Displacement field again rearranged

$$\begin{aligned}\bar{u} &= u + z\psi_x - z^3\frac{4}{3h^2}\left(\frac{\partial w}{\partial x} + \psi_x\right) = u + f_1(z)\psi_x + f_2(z)\frac{\partial w}{\partial x}\\ \bar{v} &= v + z\psi_y - z^3\frac{4}{3h^2}\left(\frac{\partial w}{\partial y} + \psi_y\right) = u + f_1(z)\psi_y + f_2(z)\frac{\partial w}{\partial y}\\ \bar{w} &= w;\end{aligned} \quad (13)$$

Where, $f_1(z) = C_1 z - C_2 z^3$; $f_2(z) = C_4 z^3$;

$$C_1 = 1, C_4 = C_2 = \frac{4}{3h^2}; \quad (14)$$

From Eq. (13), it is seen that the expressions for in-plane displacement $\bar{u}$ and $\bar{v}$ involve the derivatives of out of plane displacement w. As a result of this, second order derivatives would be present in the strain vector, thus necessitating the employment of C^1 continuity for finite element analysis. The complexity and difficulty involved with making a choice of C^1 continuity are well known.

Expressing the displacement field in the following form avoids this

$$\begin{aligned}\bar{u} &= u + f_1(z)\psi_x + f_2(z)\theta_x = u + f_1(z)\psi_1 + f_2(z)\theta_1\\ \bar{v} &= v + f_1(z)\psi_y + f_2(z)\theta_y = u + f_1(z)\psi_2 + f_2(z)\theta_2\\ \bar{w} &= w;\end{aligned} \quad (15)$$

Where, $\frac{\partial w}{\partial x} = \theta_x = \theta_1$; $\frac{\partial w}{\partial y} = \theta_y = \theta_2$

It can be seen that the number of degrees of freedom (DOF) per node, by treating θ_x and θ_y as separate DOFs, increases from 5 to 7 for HSDT model. However, the strain vector will be having only first order derivatives, and hence a C^0 continuous element would be sufficient for the finite element analysis (Reddy 1984).

3.2 Strain displacement relation

By assuming small deformation, the linear strain vectors corresponding to displacement fields are,

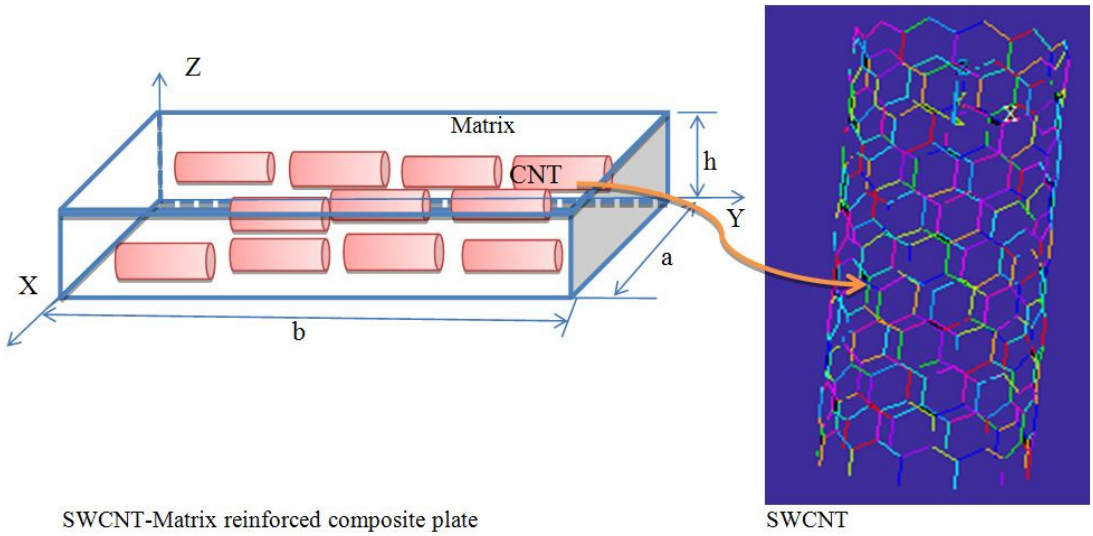

Fig. 2 Geometry of the straight aligned SWCNT R composite plate

$$\{\varepsilon\} = \{\varepsilon_1, \varepsilon_2, \varepsilon_3, \varepsilon_4, \varepsilon_5, \varepsilon_6\}^T \tag{16}$$

Where, $\varepsilon_i^0 (i = 1, 2..., 6)$ and $k_i^0 (i = 1, 2..., 6)$ are mid-plane strains and curvatures and are given by

$$\begin{aligned}
\varepsilon_1 &= \varepsilon_1^o + z(\mathrm{k}_1^o + \mathrm{z}^2\mathrm{k}_1^2)\ ;\\
\varepsilon_2 &= \varepsilon_2^o + z(\mathrm{k}_2^o + \mathrm{z}^2\mathrm{k}_2^2)\ ;\\
\varepsilon_4 &= \varepsilon_4^o + \mathrm{z}^2\mathrm{k}_4^2\ ;\\
\varepsilon_5 &= \varepsilon_5^o + \mathrm{z}^2\mathrm{k}_5^2\ ;\\
\varepsilon_6 &= \varepsilon_6^o + z(\mathrm{k}_6^o + \mathrm{z}^2\mathrm{k}_6^2)\ ;
\end{aligned} \tag{17}$$

Where

$$\varepsilon_1^o = \frac{\partial u}{\partial x}, \quad \mathrm{k}_1^o = \frac{\partial \psi_x}{\partial x}; \quad \mathrm{k}_1^2 = -\frac{4}{3h^2}\left(\frac{\partial^2 w}{\partial x^2} + \frac{\partial \psi_x}{\partial x}\right)$$

$$\varepsilon_2^o = \frac{\partial u}{\partial y}, \quad \mathrm{k}_2^o = \frac{\partial \psi_y}{\partial y}; \quad \mathrm{k}_2^2 = -\frac{4}{3h^2}\left(\frac{\partial^2 w}{\partial y^2} + \frac{\partial \psi_y}{\partial y}\right)$$

$$\varepsilon_6^o = \frac{\partial u}{\partial x} + \frac{\partial v}{\partial y}, \quad \mathrm{k}_6^o = \frac{\partial \psi_x}{\partial y} + \frac{\partial \psi_y}{\partial x};$$

$$\mathrm{k}_6^2 = -\frac{4}{3h^2}\left(\frac{\partial \psi_x}{\partial y} + \frac{\partial \psi_y}{\partial x} + 2\frac{\partial^2 w}{\partial xy}\right)$$

$$\varepsilon_4^o = \psi_y + \frac{\partial w}{\partial y}, \mathrm{k}_4^2 = -\frac{4}{h^2}\left(\psi_y + \frac{\partial w}{\partial y}\right)$$

$$\varepsilon_5^o = \psi_x + \frac{\partial w}{\partial x}, \mathrm{k}_5^2 = -\frac{4}{h^2}\left(\psi_x + \frac{\partial w}{\partial x}\right)$$

Here, the mid-plane strain vector can be written as

$$\{\bar{\varepsilon}\} = \left(\varepsilon_1^0 \ \ \varepsilon_2^0 \ \ \varepsilon_6^0 \ \ k_1^0 \ \ k_2^0 \ \ k_6^0 \ \ k_1^2 \ \ k_2^2 \ \ k_6^2 \ \ \varepsilon_4^0 \ \ \varepsilon_5^0 \ \ k_4^2 \ \ k_5^2\right), \tag{18}$$

The mid-plane displacement vector for the modified c_0 continuous model can be written as

$$q = \left\{\mathrm{u\ v\ w}\ \theta_y\ \theta_x\ \ \psi_y\ \psi_x\right\}^T \tag{19}$$

3.3 Constitutive equation (*Stress-strain relation*)

Stress is related to strain by following relation

$$\{\sigma\} = \left[\bar{Q}\right]\{\varepsilon\} \tag{20}$$

The stress vector by considering $\sigma_z = 0$ and $\varepsilon_z = 0$ can rewrite as

$$\begin{Bmatrix}\sigma_x\\ \sigma_y\\ \tau_{xy}\\ \tau_{yz}\\ \tau_{xz}\end{Bmatrix} = \begin{Bmatrix}\sigma_1\\ \sigma_2\\ \tau_6\\ \tau_4\\ \tau_5\end{Bmatrix} = \begin{bmatrix}\bar{Q}_{11} & \bar{Q}_{12} & \bar{Q}_{16} & 0 & 0\\ \bar{Q}_{12} & \bar{Q}_{22} & \bar{Q}_{26} & 0 & 0\\ \bar{Q}_{16} & \bar{Q}_{26} & \bar{Q}_{66} & 0 & 0\\ 0 & 0 & 0 & \bar{Q}_{44} & \bar{Q}_{45}\\ 0 & 0 & 0 & \bar{Q}_{45} & \bar{Q}_{55}\end{bmatrix}\begin{Bmatrix}\varepsilon_x\\ \varepsilon_y\\ \gamma_{xy}\\ \gamma_{yz}\\ \gamma_{xz}\end{Bmatrix} \tag{21}$$

where

$[\bar{\mathrm{Q}}] = \begin{bmatrix}\bar{Q}_{11} & \bar{Q}_{12} & \bar{Q}_{16} & 0 & 0\\ \bar{Q}_{12} & \bar{Q}_{22} & \bar{Q}_{26} & 0 & 0\\ \bar{Q}_{16} & \bar{Q}_{26} & \bar{Q}_{66} & 0 & 0\\ 0 & 0 & 0 & \bar{Q}_{44} & \bar{Q}_{45}\\ 0 & 0 & 0 & \bar{Q}_{45} & \bar{Q}_{55}\end{bmatrix}$ is the elasticity matrix.

Where

$$\begin{aligned}
\bar{Q}_{11} &= Q_{11}\cos^4\theta_k + Q_{22}\sin^4\theta_k + 2(Q_{12} + 2Q_{66})\sin^2\theta_k\cos^2\theta_k,\\
\bar{Q}_{12} &= (Q_{11} + Q_{22} - 4Q_{66})\sin^2\theta_k\cos^2\theta + Q_{12}\left(\cos^4\theta_k + \sin^4\theta_k\right),\\
\bar{Q}_{22} &= Q_{22}\cos^4\theta_k + Q_{11}\sin^4\theta_k + 2(Q_{12} + 2Q_{66})\sin^2\theta_k\cos^2\theta_k,\\
\bar{Q}_{16} &= (Q_{11} - Q_{12} - 2Q_{66})\sin\theta_k\cos^3\theta_k + (Q_{12} - Q_{22} + 2Q_{66})\sin^3\theta_k\cos\theta_k,\\
\bar{Q}_{26} &= (Q_{11} - Q_{12} - 2Q_{66})\sin^3\theta_k\cos\theta_k + (Q_{12} - Q_{22} + 2Q_{66})\sin\theta_k\cos^3\theta_k,\\
\bar{Q}_{44} &= Q_{44}\cos^2\theta_k + Q_{55}\sin^2\theta_k,\\
\bar{Q}_{45} &= (Q_{55} - Q_{44})\sin\theta_k\cos\theta_k = \bar{Q}_{54},\\
\bar{Q}_{55} &= Q_{55}\cos^2\theta_k + Q_{44}\sin^2\theta,\\
\bar{Q}_{66} &= (Q_{11} + Q_{22} - 2Q_{12} - 2Q_{66})\mathrm{si,n}^2\theta_k\cos^2\theta_k + Q_{66}\left(\cos^4\theta_k + \sin^4\theta_k\right),
\end{aligned}$$

3.4 Finite Element Methods (*FEM*)

The finite element method (FEM) is a numerical technique being used for finding an approximate solution to a wide variety of engineering problems through bending Approach. In the present paper eight nodded isoperimetric elements with seven degree of freedom per node is employed for finite element plate modeling.

$$q = \sum_{i=1}^{NN} N_i q_i; \qquad x = \sum_{i=1}^{NN} N_i x_i\ ; \qquad y = \sum_{i=1}^{NN} N_i y_i \tag{22}$$

Where, N_i and q_i are the interpolation function and vector of unknown displacements for the i^{th} node, respectively, NN is the number of nodes per element and x_i and y_i are Cartesian coordinate of the i^{th} node. The strain are related to displacement by strain-displacement matrix $[B_i]$

$$\left\{\bar{\varepsilon_l}\right\}_{13\times 1} = \left[B_i\right]_{13\times 7}\{\mathrm{N}_i\}_{7\times 1} \tag{23}$$

$$\left\{\bar{\varepsilon_l}\right\} = \begin{Bmatrix}\varepsilon_1^0\\ \varepsilon_2^0\\ \varepsilon_6^0\\ k_1^0\\ k_2^0\\ k_6^0\\ k_1^2\\ k_2^2\\ k_6^2\\ \varepsilon_4^0\\ \varepsilon_5^0\\ k_4^2\\ k_5^2\end{Bmatrix} = \begin{bmatrix}\partial/\partial x & 0 & 0 & 0 & 0 & 0 & 0\\ 0 & \partial/\partial y & 0 & 0 & 0 & 0 & 0\\ \partial/\partial y & \partial/\partial x & 0 & 0 & 0 & 0 & 0\\ 0 & 0 & 0 & 0 & 0 & 0 & C1\partial/\partial x\\ 0 & 0 & 0 & 0 & 0 & C1\partial/\partial y & 0\\ 0 & 0 & 0 & 0 & 0 & C1\partial/\partial x & C1\partial/\partial y\\ 0 & 0 & 0 & 0 & -C4\partial/\partial x & 0 & -C2\partial/\partial x\\ 0 & 0 & 0 & -C4\partial/\partial y & 0 & -C2\partial/\partial y & 0\\ 0 & 0 & 0 & -C4\partial/\partial x & -C4\partial/\partial y & -C2\partial/\partial x & -C2\partial/\partial y\\ 0 & 0 & C1\partial/\partial y & 0 & 0 & C1 & 0\\ 0 & 0 & C1\partial/\partial x & 0 & 0 & 0 & C1\\ 0 & 0 & 0 & -3C4 & 0 & -3C2 & 0\\ 0 & 0 & 0 & 0 & -3C4 & 0 & -3C2\end{bmatrix}\begin{Bmatrix}u\\ v\\ w\\ \theta_y\\ \theta_x\\ \psi_y\\ \psi_x\end{Bmatrix},$$

The elemental stiffness matrices $[k^e]$ can be expressed as

$$\left[k^e\right] = \int_{A^e}\{B\}^T[D]\{B\}\,dA \tag{24a}$$

Where, $[D]$ is a material property matrix, defined as

$$D=\sum_{k=1}^{NL}\int_{z_{k-1}}^{z_k}[T]^T\left[\bar{Q}_{ij}\right][T]dz$$
$$=\begin{bmatrix}[A_1] & [B] & [E] & 0 & 0\\ [B] & [C_1] & [F_1] & 0 & 0\\ [E] & [F_1] & [H] & 0 & 0\\ 0 & 0 & 0 & [A_2] & [C_2]\\ 0 & 0 & 0 & [C_2] & [F_2]\end{bmatrix} \quad (24b)$$

With

$$\left(A_{ij},\ B_{ij},\ C_{1ij},\ E_{ij},\ F_{1ij},\ H_{ij}\right)=\sum_{k=1}^{NL}\int_{z_{k-1}}^{z_k}\bar{Q}_{ij}^{(k)}\left(1,\ z,\ z^2,\ z^3,\ z^4,\ z^6\right)dz, \quad (25)$$

For $i, j = 1, 2, 6$

$$\left(A_{2ij},\ C_{2ij},\ F_{2ij},\right)=\sum_{k=1}^{NL}\int_{z_{k-1}}^{z_k}\bar{Q}_{ij}^{(k)}\left(1\quad z\quad z^4\right)dz \quad (26)$$

The elemental stiffness matrix in natural coordinate system (ξ, η) can be expressed as

$$\left[k^e\right]=\int_{-1}^{1}\int_{-1}^{1}[B]^T[D][B]\det[J]d\xi d\eta \quad (27)$$

Where, the jacobian [J] is

$$[J]=\begin{bmatrix}\frac{dx}{d\xi} & \frac{dy}{d\xi}\\ \frac{dx}{d\eta} & \frac{dy}{d\eta}\end{bmatrix}$$

3.5 Potential energy of the SWCNTRC plate

The total potential energy of SWCNTRC plate is sum of potential energy due to internal strain energy U_1 and potential energy due to external applied loading U_2 and given by

$$U_1^e=\sum_{e=1}^{NE}U_1^e-\sum_{e=1}^{NE}U_2^e \quad (28)$$

The internal potential energy in the form of strain energy is given by using Eqs. (18) and (24)

$$U_1^e=\frac{1}{2}\int_{A^e}[\bar{\varepsilon}]^T\{[D]\}[\bar{\varepsilon}]dA \quad (29)$$

The mid-plain strain $\{\bar{\varepsilon}\}$ can be can written in terms of displacement as

$$\left\{\bar{\varepsilon}\right\}_{13\times1}=\left[B_i\right]_{13\times7}\left\{\mathrm{N}_i\right\}_{7\times1} \quad (30)$$

Using Eqs. (30) and (29) can be obtained

$$U_1^e=\frac{1}{2}\int_{A^e}\{q\}^T[B_i]^T[D][B_i]\{q\}[\bar{\varepsilon}]dA \quad (31)$$

Substituting Eq. (22) in Eq. (31) we obtained

$$U_1^e=\frac{1}{2}\int_{A^e}\left\{\left(\sum_{i=1}^{NN}\{q_i\}^T[B_i]N_i\right)[D]\left(\sum_{i=1}^{NN}\{q_i\}[B_i]N_i\right)\right\}dA \quad (32)$$

Using Eq. (23), we get

$$U_1^e=\frac{1}{2}\int_{A^e}\{q\}^T[B][D][B]\{q\}\,dA \quad (33)$$

Where, q is a generated displacement vector for the SWCNTRC plate. The elemental potential energy due to external applied loading is given by

$$U_2^e=\int_A\{q\}^T\left[\bar{F}\right]dA \quad (34)$$

Where, $[\bar{F}]$ is load vector corresponds to each DOF. For the present case sinusoidal distributed transverse load $[\bar{F}]$ can be written as

$$\{\bar{\mathrm{F}}\}=\begin{Bmatrix}0 & 0 & P & 0 & 0 & 0 & 0\end{Bmatrix}^T \quad (35)$$

Where, $P(\mathrm{x},\mathrm{y})=q_0\sin\left(\frac{\pi x}{a}\right)\sin\left(\frac{\pi y}{b}\right)$.

Substituting for $\{q\}$ form Eq. (22) in Eq. (34) we obtained

$$U_2^e=\int_{A^e}\left(\sum_{i=1}^{NN}\{q_i\}^T N_i\right)\left\{\bar{F}_i^{(e)}\right\}^T dA$$
$$U_2^e=\left\{q^{(e)}\right\}^T\left\{F^{(\mathrm{e})}\right\} \quad (36)$$

Where

$$\left\{F^{(\mathrm{e})}\right\}=\int_{A^e}\{N\}^e\left\{\bar{F}\right\}^e dA$$

The equilibrium Equation governing the present problem for the SWCNTRC plate can obtain by minimizing potential energy with respect to displacement. Substituting Eqs. (33) and (36) in Eq. (28) and minimizing with respect to $\{q\}$, we obtained

$$\{F_i\}=[\mathrm{K}_{ij}]\{q_i\} \quad (37)$$

Where, $\{F_i\}=-\sum_{e=1}^{NE}\{F\}^e$ is global force vector, $\left[K_{ji}\right]=\sum_{e=1}^{NE}\left[K_{ij}^e\right]$ is global stiffness matrix, $\{q_i\}=\sum_{e=1}^{NE}\{q\}^e$ is global displacement vector.

Eq. (37) is then solved for SWCNTRC plate acted upon by various transverse loadings to obtained displacement.

4. Numerical result and discussion

A finite element code has been developed in MATLAB [R2013a] based on HSDT, for implementing bending analysis of SWCNTRC-FG plate acted upon by sinusoidal transverse loading conditions. The SWCNTRC plate is discretized by using an eight noded quadratic isoperimetric

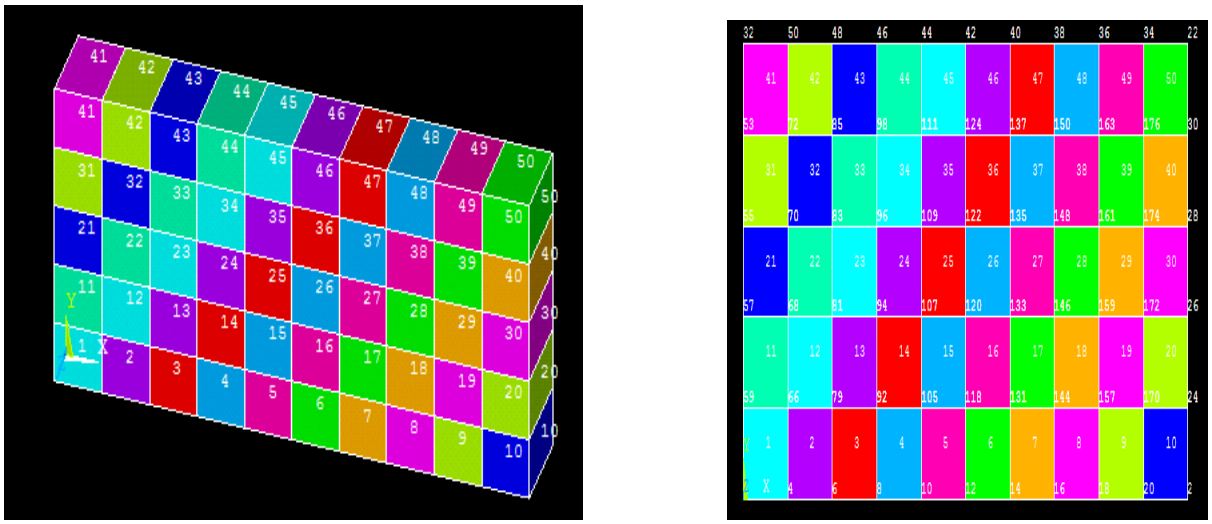

Fig. 3 SWCNTRC plate discretized by using 8 noded quadratic isoperimetric elements

Table 1 Elastic properties of SWCNT is taken from Herasati *et al*. (2014)

Chirality index	E_{22}, E_{33} (GPa)	E_{11} (GPa)	G_{12} (GPa)	v_{12}, v_{21}	v_{23}
(5, 5)	5.11	58.64	1.605	0.33	0.48
(10, 10)	6.05	103.23	2.11	0.33	0.51
(15, 15)	5.75	131.8	2.49	0.32	0.63
(20, 20)	4.17	158.24	2.79	0.32	0.78

element with 56 DOFs per element as shown in Fig. 3. Here, EPON-862 is selected for the matrix which have elastic constant E_m = 3.0215 GPa v_m = 0.3 respectively. In addition SWCNTs are selected as reinforcements with material properties listed in Table 1. The effective elastic properties of SWCNTRC plate is calculated by Eq. (7). The transverse loading conditions. The SWCNTRC plate is discretized by using an eight noded quadratic isoperimetric element with 56 DOFs per element as shown in Fig. 3. Here, EPON-862 is selected for the matrix which have elastic constant E_m = 3.0215 GPa v_m = 0.3 respectively. In addition SWCNTs are selected as reinforcements with material properties listed in Table 1. The effective elastic properties of SWCNTRC plate is calculated by Eq. (7). The geometrical properties of SWCNRC plate a = 5 mm, b = 10 mm, h = 0.356 mm is considered of further analysis as shown in Fig. 2.

The various boundary conditions are considered for present analysis and also can be represented as:

(a) All edge is simply supported edges (SSSS)

$$u = v = w = \psi_y = \theta_y = 0 \quad \text{at} \quad x = 0 \quad \text{and} \quad a;$$

$$u = v = w = \psi_x = \theta_x = 0 \quad \text{at} \quad y = 0 \quad \text{and} \quad b.$$

(b) All is edge clamped (CCCC)

$$u = v = w = \psi_x = \psi_y = \theta_x = \theta_y = 0$$

at $x = 0, a$ and $y = 0, b$

Table 2 Non-dimensional central displacement for CNT reinforced composite plate subjected to uniform transverse load with volume fraction of SWCNT (V_{CNT})

		SSSS		CCCC		CFCF		CFFF	
V_{CNT}		Lei *et al*. (2016)	Present	Lei *et al*. (2016)	Present	Lei *et al*. (2016)	Present	Lei *et al*. (2016)	Present
0.11	UD	7.3234	7.3200	3.8306	3.8306	5.4371	5.4370	28.6211	28.6210
	FG-V	7.3165	7.3095	3.8332	3.8032	5.4327	5.4320	28.6908	28.6808
	FG-O	7.3982	7.3985	3.8440	3.8440	5.4488	5.4488	28.77703	28.7875
	FG-X	7.2150	7.2087	3.7889	3.7889	5.4135	5.4030	28.335	28.3540
0.14	UD	6.3455	6.3454	3.5060	3.5142	5.0539	5.0654	24.8896	24.8972
	FG-V	6.3264	6.3250	3.4965	3.4965	5.0505	5.0505	24.8831	24.8831
	FG-O	6.3955	6.3950	3.5153	3.4853	5.0840	5.0850	24.9450	24.9442
	FG-X	6.2405	6.2015	3.4590	3.4590	5.0352	5.0354	24.6011	24.6011
0.17	UD	4.7024	4.5871	2.4289	2.4289	3.4210	3.4224	18.3666	18.3666
	FG-V	4.678	4.564	2.4221	2.4220	3.4181	3.4178	18.3356	18.3587
	FG-O	4.7314	4.7315	2.4365	2.4365	3.4544	3.4588	18.3871	18.3871
	FG-X	4.6117	4.6117	2.3931	2.3931	3.4054	3.4054	18.1007	18.1007

Table 3 Non-dimensional central displacements for CNT reinforced composite plate subjected to uniform transverse load with different width-to-thickness ratio (a/h)

		SSSS		CCCC		CFCF		CFFF	
a/h		Lei *et al*. (2016)	Present	Lei *et al*. (2016)	Present	Lei *et al*. (2016)	Present	Lei *et al*. (2016)	Present
10	UD	7.3234	7.3234	3.8306	3.8006	5.4371	5.4370	28.6211	28.621
	FG-V	7.3165	7.3254	3.8332	3.8332	5.4327	5.4327	28.6908	28.690
	FG-O	7.3982	7.3980	3.8440	3.8570	5.4488	5.4489	28.7703	28.7703
	FG-X	7.2150	7.2150	3.78889	3.7898	5.4135	5.4136	28.3350	28.3350
20	UD	4.8928	4.8928	1.6495	1.6495	1.9832	1.9000	18.1915	18.1920
	FG-V	4.8962	4.8960	1.6581	1.6542	1.9850	1.8790	18.3139	18.3254
	FG-O	4.9657	4.9658	1.6659	1.5866	1.9895	1.9894	18.3932	18.4065
	FG-X	4.8100	4.8122	1.6255	1.6055	1.9653	1.9653	17.9591	17.9590
50	UD	4.1634	4.1634	0.9596	0.9596	1.0156	1.0154	15.2643	15.2645
	FG-V	4.1702	4.1875	0.9687	0.9687	1.0224	1.2265	15.4013	15.4016
	FG-O	4.2359	4.2395	0.9748	0.9747	1.0269	1.0296	15.4807	15.4807
	FG-X	4.0887	4.0897	0.9431	0.9431	1.0026	1.0026	15.0470	15.0458

(c) Two opposite edges clamped and other two simply supported (CSCS)

$$u = v = w = \psi_x = \psi_y = \theta_x = \theta_y = 0; \text{ at } x = 0 \text{ and } y = 0$$

$$u = w = \psi_y = \theta_y = 0 \quad \text{at} \quad x = a \quad \text{and}$$

$$u = w = \psi_x = \theta_x = 0 \quad \text{at} \quad y = b$$

Tables 2-3 shows the central deflection of a square SWCNTRC-FG plate subjected to sinusoidal transvers loading for different volume fraction of CNT. The bending response of SWCNTRC plate using present approach is compared with the results of the various literatures. It is observed from the results that for thick SWCNTRC plates (a/h < 20), the response obtained by using present approach shows close proximity with the 3D elastic solution. As all the commercial software codes such as ABAQUS and ANSYS are based on FSDT/CLPT, but present bending analysis problem, a MATLAB code based on HSDT is developed for accurate computation of deflection and stress. The results obtained by a present finite element code, developed in MATLAB, validated with the results available in literatures, Lei *et al*. (2016). It is found from these validation studies that the results show good agreement with the results available in the literature.

Fig. 4 shows the effect of the (a/h) on the deflection for SWCNTRC-FG plates subjected to sinusoidal loading (P). The results are obtained by utilizing a proposed bending analysis based on HSDT theory. The non-dimensional central deflection decreased with increasing a/h; however, FG-X and FG-V plates are stiffer than the other pate

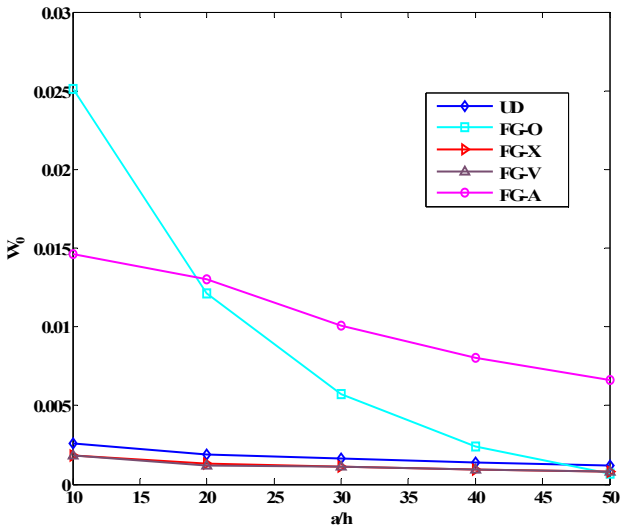

Fig. 4 Non-dimensional central deflections (W_0) versus width-to-thickness ratio for SWCNTRC-FG plate subjected to sinusoidal loading

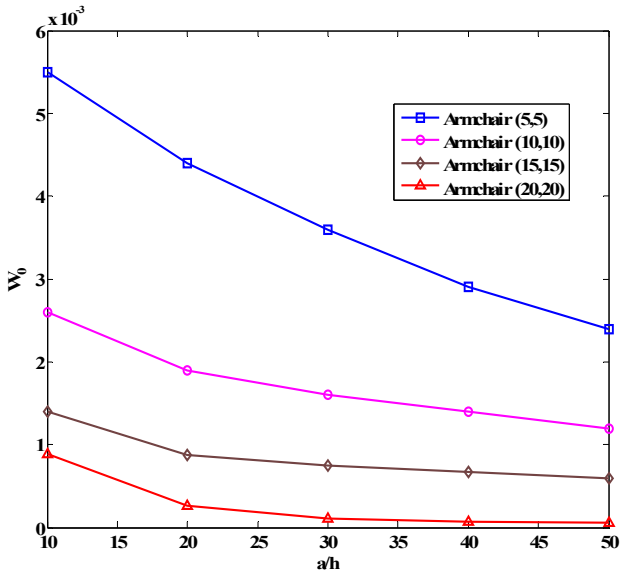

Fig. 5 Non-dimensional central deflection (W_0) versus width-to-thickness ratio (a/h) for different SWCNT configuration of plate subjected to sinusoidal transvers loading

structure while FG-O plate is weaker. Fig. 5 non-dimensional central deflection (W_0) versus width-to-thickness ratio for different SWCNT configuration of plate subjected to sinusoidal transvers loading (P). The results clearly show that the non-dimensional central deflection of Armchair (5, 5) CNT gives maximum as compare to the other configuration of SWCNTRC plates. It is clear that, Armchair (20, 20) plate is stronger than other configuration of plates. Fig. 6 depicts the non-dimensional central deflection versus volume fraction of SWCNT for different

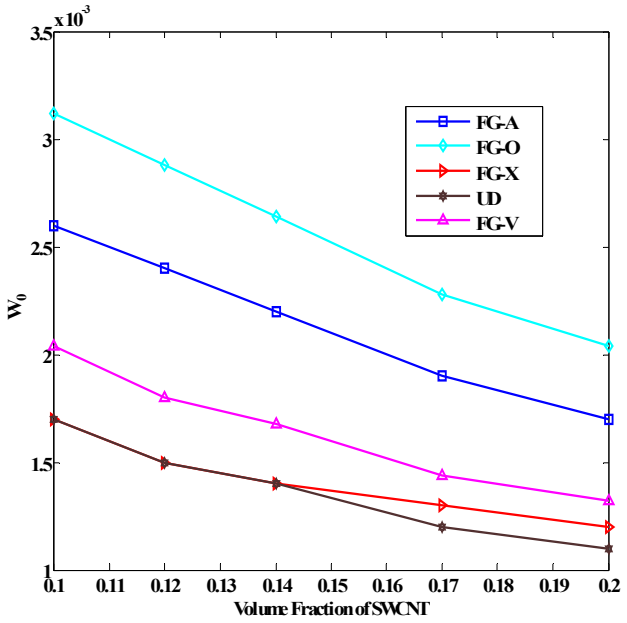

Fig. 6 Non-dimensional central deflection (W_0) versus volume fraction of SWCNT for different SWCNTRC-FG of plate subjected to sinusoidal transvers loading

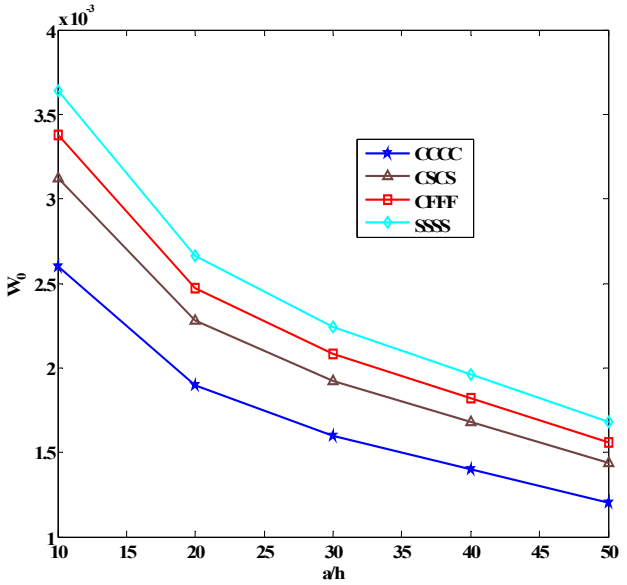

Fig. 7 Non-dimensional central deflection (W_0) versus a/h for different boundary condition of SWCNTRC-FG plate subjected to sinusoidal transvers loading

SWCNTRC-FG plates subjected to sinusoidal transvers loading (P). It can be observed that the central deflection of SWCNTRC-FG plate decreased with increasing volume fraction of SWCNT. The reinforcement increased than structure become stronger. Fig. 7 shows non- dimensional central deflection (W_0) versus a/h ratio for different boundary condition of plate subjected to sinusoidal transvers loading (P). It is observed that central deflection decreased with increasing a/h ratio. The CCCC boundary condition is stiffer than the other types of boundary condition of SWCNTRC plates. Fig. 8 depicts variation of in-plane normal stresses (σ_x) through thickness (z/h) of simply supported boundary condition SWCNTRC plate subjected to sinusoidal transvers loading. It can be found hat the central normal stress distribution in SWCNTRC plates is anti-symmetric about the mid-plane due to

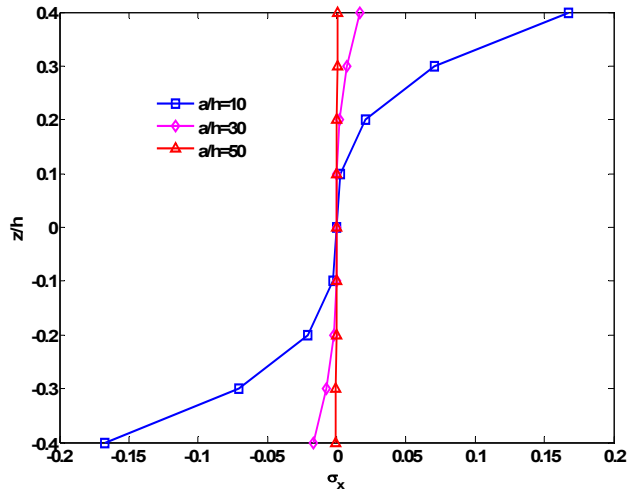

Fig. 8 Variation of in-plane normal stresses (σ_x) through thickness (z/h) of simply supported boundary condition SWCNTRC plate subjected to sinusoidal transvers loading

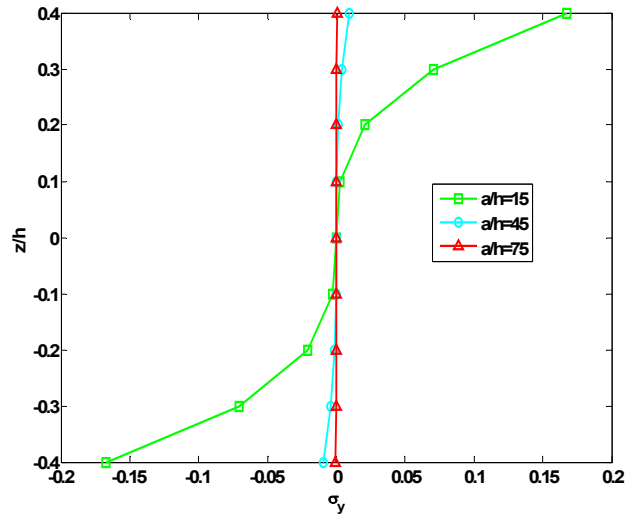

Fig. 9 Variation of in-plane normal stresses (σ_y) through thickness (z/h) of simply supported boundary condition SWCNTRC plate subjected to sinusoidal transvers loading

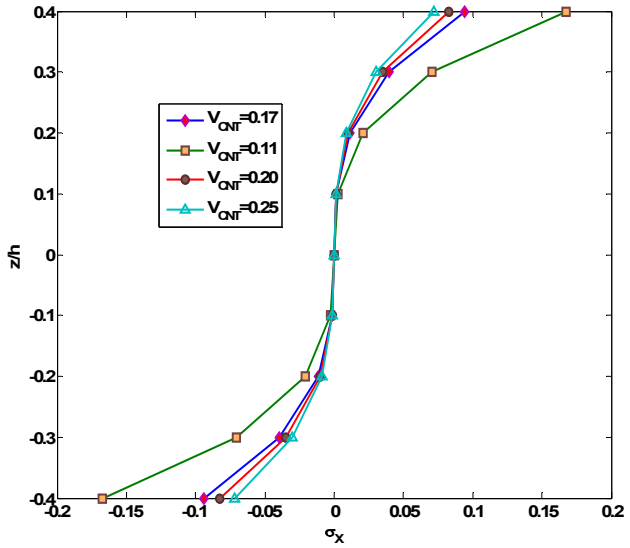

Fig. 10 Variation of in-plane normal stresses (σ_x) through thickness (z/h) of simply supported boundary condition SWCNTRC plate subjected to sinusoidal transvers loading

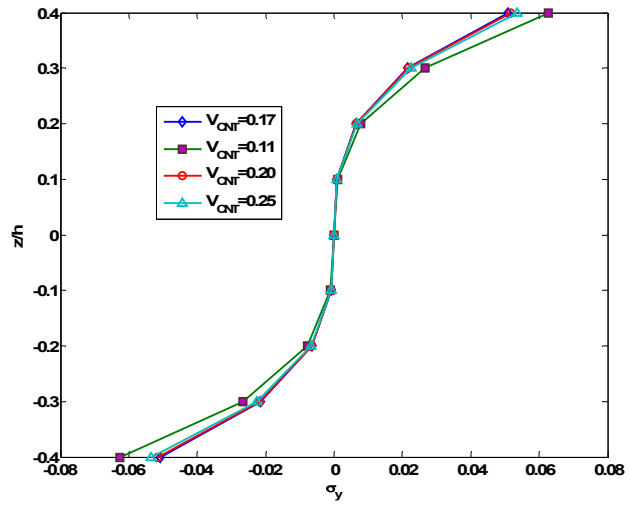

Fig. 11 Variation of in-plane normal stresses (σ_y) through thickness (z/h) of simply supported boundary condition SWCNTRC plate subjected to sinusoidal transvers loading

thexsymmetric reinforcement with respect to the mid-plane. Fig. 9 shows variation of in-plane normal stresses (σ_y) through thickness (z/h) of simply supported boundary condition SWCNTRC plate subjected to sinusoidal transvers loading. It can be seen that stresses decreased with increasing a/h ratio. Fig. 10 depicts variation of in-plane normal stresses (σ_x) through thickness (z/h) of simply supported boundary condition SWCNTRC plate subjected to sinusoidal transvers loading. It can be found that the central normal stress distribution in SWCNTRC plates is anti-symmetric about the mid-plane due to the symmetric reinforcement with respect to the mid-plane. Fig. 11 shows the non-dimensional central normal stresses σ_y distributed along the non-dimensional thickness (z/h) of various

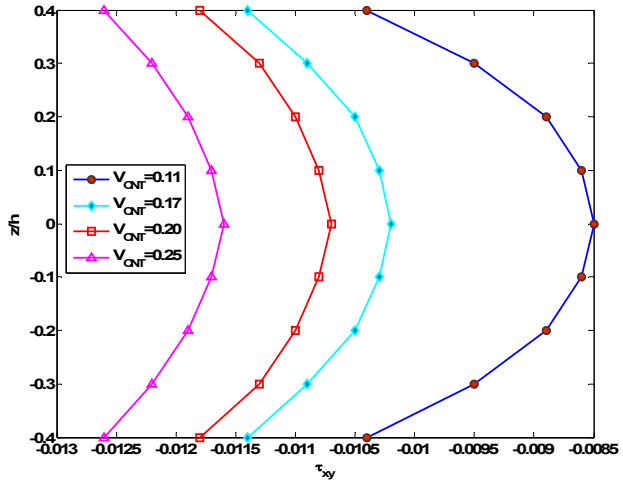

Fig. 12 Variation of shear stresses (τ_{xy}) through thickness (z/h) of simply supported boundary condition SWCNTRC plate subjected to sinusoidal transvers loading

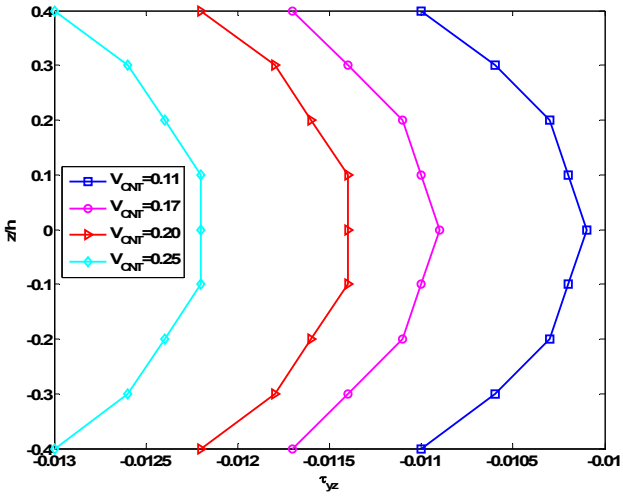

Fig. 13 Variation of shear stresses (τ_{yz}) through thickness (z/h) of simply supported boundary condition SWCNTRC plate subjected to sinusoidal transvers loading

volume fraction of SWCNTRC plate with four edge simply supported subjected to sinusoidal transverse load (P) with a/h = 50. It can be found that the central normal stress distribution in SWCNTRC plate is anti-symmetric about the mid-plane due to the symmetric reinforcement with respect to the mid-plane. Fig. 12 shows the non-dimensional central shear stresses τ_{xy} distributed along the non-dimensional thickness (z/h) of various volume fraction of SWCNTRC plate with four edge simply supported subjected to sinusoidal transverse load (P) with a/h = 50. It can be seen that maximum shear stress at thickness (z/h) = 0. Fig. 13 presents the non-dimensional central shear stresses τ_{yz} distributed along the non-dimensional thickness (z/h) of various volume fraction of SWCNTRC plate with four edge simply supported subjected to sinusoidal transverse load (P) with a/h = 50. It can be seen that shear stress decreased with increasing volume fraction of SWCNT. Fig. 14 shows the

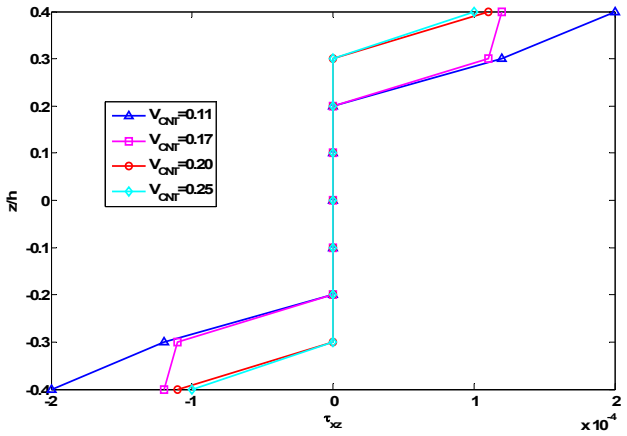

Fig. 14 Variation of shear stresses (τ_{xz}) through thickness (z/h) of simply supported boundary condition SWCNTRC plate subjected to sinusoidal transvers loading

non-dimensional central shear stresses τ_{xy} distributed along the non-dimensional thickness (z/h) of various volume fraction of SWCNTRC plate with four edge simply supported subjected to sinusoidal transverse load (P) with a/h = 50. It can be found that the central shear stress distribution in SWCNTRC plate is anti-symmetric about the mid-plane due to the symmetric reinforcement with respect to the mid-plane.

5. Conclusions

In this study, the bending behavior of the SWCNT reinforced composite plate of five different grading (UD, FG-X, FG-O,FG-A and FG-V) under sinusoidal transverse loading have been examined using the HSDT kinematic model. The SWCNTRC-FG plate is embedded of perfect bonded Epon-862 matrix. The SWCNT is assumed to be functionally graded in the thickness direction. The structure is graded functionally through the thickness based on the volume fractions of the CNT, and the effective properties are evaluated through the micromechanical model using the Mori-Tanaka. The desired governing equation for the bending analysis is obtained using minimum potential energy principle and discretized through the suitable isoperimetric finite element steps. The model has also been validated by comparing the responses to results available in the literature. The applicability of the present higher-order model has been highlighted by computing the responses for the different geometrical and material parameters.

Following points are concluded

- The close agreement between the results obtained by the present approach and those appearing in the published literature establishes the correctness of the formulation.
- Non dimensional Central deflection of SWCNTRC plate is decreased with increasing width-to-thickness ratio (a/h).
- Non dimensional Central deflection of SWCNTRC plate is decreased with increasing volume fraction of SWCNT (V_{CNT}).
- FG-X plate is more stiffer than the other types of plate
- The maximum displacement present in armchair (5, 5) as compared to other configuration SWCNT.
- The minimum displacement present for CCCC boundary condition as compared to other boundary condition.

References

Bakhti, K., Kaci, A., Bousahla, A.A., Houari, M.S.A., Tounsi, A. and Adda Bedia, E.A. (2013), "Large deformation analysis for functionally graded carbon nanotube-reinforced composite plates using an efficient and simple refined theory", *Steel Compos. Struct., Int. J.*, **14**(4), 335-347.

Bhashyam, G.R. and Gallagher, R.H. (1983), "A triangular shear-flexible finite element for moderately thick laminated composite plates", *Comput. Methods Appl. Mech. Eng.*, **40**(3), 309-326.

Bounouara, F., Benrahou, K.H., Belkorissat, I. and Tounsi, A. (2016), "A nonlocal zeroth-order shear deformation theory for free vibration of functionall1

y graded nanoscale plates resting on elastic foundation", *Steel Compos. Struct., Int. J.*, **20**(2), 227-249.

Fard, K.M. (2015), "Higher order static analysis of truncated conical sandwich panels with flexible cores", *Steel Compos. Struct., Int. J.*, **19**(6), 1333-1354.

Hadianfard, M.A. and Khakzad, A.R. (2016), "Inelastic buckling and post-buckling behavior of gusset plate connections", *Steel Compos. Struct., Int. J.*, **22**(2), 411-427.

Han, Y. and Elliott, J. (2007), "Molecular dynamics simulations of the elastic properties of polymer/carbon nanotube composites", *Compute. Mater. Sci.*, **39**(2), 315-323.

Hebali, H., Bakora, A., Tounsi, A. and Kaci, A. (2016), "A novel four variable refined plate theory for bending, buckling, and vibration of functionally graded plates", *Steel Compos. Struct., Int. J.*, **22**(3), 473-495.

Herasati, S., Zhang, L.C. and Ruan, H.H. (2014), "A new method for characterizing the interphase regions of carbon nanotube composites", *Int. J. Solids Struct.*, **51**(9), 1781-1179.

Houari, M.S.A., Tounsi, A., Bessaim, A. and Mahmoud, S.R. (2013), "A new simple three-unknown sinusoidal shear deformation theory for functionally graded plates", *Steel Compos. Struct., Int. J.*, **22**(2), 257-276.

Hu, H., Onyebueke, L. and Abatan, A. (2010), "Characterizing and modeling mechanical properties of nanocomposites-review and evaluation", *J. Minerals Mater. Characteriz. Eng.*, **9**(4), 275-319.

Huang, Y.Y., Hwang, K.C. and Gao, H. (2004), "The effect of nanotube waviness and agglomeration on the elastic property of carbon nanotube-reinforced composites", *Urbana*, **51**, p. 61801.

Kara, M.E., Firat, F.K., Sonmez, M. and Karabork, T. (2016), "An investigation of anchorage to the edge of steel plates bonded to RC structures", *Steel Compos. Struct., Int. J.*, **22**(1), 25-43.

Kreculj, D.D. (2008), "Stress analysis in an unidirectional carbon/epoxy composite material", *FME Transactions*, **36**(3), 127-132.

Lei, Z.X., Liew, K.M. and Yu, J.L. (2013), "Large deflection analysis of functionally graded carbon nanotube-reinforced composite plates by the element free kp-Ritz method", *Computational Methods Applied Mechanics and Engineering*, **256**, 189-199.

Lei, Z.X., Zhang, L.W. and Liew, K.M. (2016), "Analysis of laminated CNT reinforced functionally graded plates using the

element-free kp- Ritz method", *Composites Part – B*, **84**, 211-221.
Madhu, S. and Rao, V.S. (2014), "Effect of carbon nanotube reinforcement in polymer composite plates under static loading", *Int. J. Chem. Molecul. Nuclear Mater. Metallurg. Eng.*, **8**(3), 200-205.
Mehditabar, A., Akbari Alashti, R. and Pashaei, M.H. (2014), "Magneto-thermo-elastic analysis of a functionally graded conical shell", *Steel Compos. Struct., Int. J.*, **16**(1), 77-96.
Mohammadpour, E., Awang, M., Kakooei, S. and Akil, H.M. (2014), "Modeling the tensile stress-strain response of carbon nanotube/polypropylene nanocomposite using nonlinear representative volume element", *Mater. Des.*, **58**, 36-42.
Moradi-Dastjerdi, R. and Momeni-Khabisi, H. (2016), "Dynamic analysis of functionally graded nanocomposite plates reinforced by wavy carbon nanotube", *Steel Compos. Struct., Int. J.*, **22**(2), 277-299.
Prokic, A., Lukic, D., Ladjinovic, Dj. (2014), "Automatic analysis of thin-walled laminated composite sections", *Steel Compos. Struct., Int. J.*, **16**(3), 233-252.
Rastgaar Aagaah, M., Nakhaie Jazar, G., Nazari, G. and Alimi, M. (2014), "Third order shear deformation theory for modeling of laminated composite plate", *SEMX International Congress and Exposition on Experimental and Applied Mechanics*, Costa Mesa, CA, USA, June.
Reddy, J.N. (1984), "A simple higher-order theory for laminated composite plates", *ASME J Appl Mech*, **51**(4), 745-152.
Reddy, B.S., Reddy, A.R., Kumar, J.S. and Reddy, K.V.K. (2012), "Bending analysis of laminated composite plates using finite element method", *Int. J. Eng. Sci. Technol.*, **4**(2), 177-190.
Rupp, J., Sezen, H. and Chaturvedi, S. (2014), "Axial behavior of steel-jacketed concrete columns", *Steel Compos. Struct., Int. J.*, **16**(1), 61-67.
Salami, S.J. (2016), "Extended high order sandwich panel theory for bending analysis of sandwich beams with carbon nanotube reinforced face sheets", *Physica E*, **76**, 187-197.
Sarvestani, H.Y. and Hojjati, M. (2016), "A high-order analytical method for thick composite tubes", *Steel Compos. Struct., Int. J.*, **21**(4), 755-773.
Thirumalaiselvi, A., Anandavalli, N., Rajasankar, J. and Iyer, N.R. (2016), "Numerical evaluation of deformation capacity of laced steel-concrete composite beams under monotonic loading", *Steel Compos. Struct., Int. J.*, **20**(1), 167-184.
Wattanasakulpong, N. and Chaikittiratana, A. (2015), "Exact solutions for static and dynamic analyses of carbon nanotube-reinforced composite plates with Pasternak elastic foundation", *Appl. Math. Model.*, **39**(18), 5459-5472.
Wu, Y.T., Kang, D.Y., Su, Y.T. and Yang, Y.B. (2016), "Seismic behavior of composite walls with encased steel truss", *Steel Compos. Struct., Int. J.*, **22**(2), 449-472.
Wuite, J. and Adali, S. (2005), "Deflection and stress behaviour of nano composite reinforced beam using a multiscale analysis", *Compos. Struct.*, **71**(3), 388-396.
Zhang, L.W., Lei, Z.X., Liew, K.M. and Yu, J.L. (2014), "Static and dynamic of carbon nanotube reinforced functionally graded cylindrical panels", *Compos. Struct.*, **111**, 205-212.
Zhu, P., Lei, Z.X. and Liew, K.M. (2012), "Static and free vibration analyses of carbon nanotube-reinforced composite plates using finite element method with first order shear deformation plate theory", *Compos. Struct.*, **94**(4), 1450-1460.